# Measurement of the decays $B \to \phi K$ and $B \to \phi K*$

B. Aubert, D. Boutigny, J.M. Gaillard, A. Hicheur, Y. Karyotakis, J.P. Lees, P. Robbe, V. Tisserand, A. Palano, G P. Chen, et al.

*BABAR*-PUB-01/11
SLAC-PUB-8823
hep-ex/0105001

# Measurement of the decays $B \to \phi K$ and $B \to \phi K^*$

## The *BABAR* Collaboration

B. Aubert,[1] D. Boutigny,[1] J.-M. Gaillard,[1] A. Hicheur,[1] Y. Karyotakis,[1] J.P. Lees,[1] P. Robbe,[1] V. Tisserand,[1] A. Palano,[2] G.P. Chen,[3] J.C. Chen,[3] N.D. Qi,[3] G. Rong,[3] P. Wang,[3] Y.S. Zhu,[3] G. Eigen,[4] P.L. Reinertsen,[4] B. Stugu,[4] B. Abbott,[5] G.S. Abrams,[5] A.W. Borgland,[5] A.B. Breon,[5] D.N. Brown,[5] J. Button-Shafer,[5] R.N. Cahn,[5] A.R. Clark,[5] Q. Fan,[5] M.S. Gill,[5] S.J. Gowdy,[5] A. Gritsan,[5] Y. Groysman,[5] R.G. Jacobsen,[5] R.W. Kadel,[5] J. Kadyk,[5] L.T. Kerth,[5] S. Kluth,[5] Yu.G. Kolomensky,[5] J.F. Kral,[5] C. LeClerc,[5] M.E. Levi,[5] T. Liu,[5] G. Lynch,[5] A.B. Meyer,[5] L.M. Mir,[5] M. Momayezi,[5] P.J. Oddone,[5] A. Perazzo,[5] M. Pripstein,[5] N.A. Roe,[5] A. Romosan,[5] M.T. Ronan,[5] V.G. Shelkov,[5] A.V. Telnov,[5] W.A. Wenzel,[5] P.G. Bright-Thomas,[6] T.J. Harrison,[6] C.M. Hawkes,[6] A. Kirk,[6] D.J. Knowles,[6] S.W. O'Neale,[6] R.C. Penny,[6] A.T. Watson,[6] N.K. Watson,[6] T. Deppermann,[7] H. Koch,[7] J. Krug,[7] M. Kunze,[7] B. Lewandowski,[7] K. Peters,[7] H. Schmuecker,[7] M. Steinke,[7] J.C. Andress,[8] N.R. Barlow,[8] W. Bhimji,[8] N. Chevalier,[8] P.J. Clark,[8] W.N. Cottingham,[8] N. De Groot,[8] N. Dyce,[8] B. Foster,[8] A. Mass,[8] J.D. McFall,[8] D. Wallom,[8] F.F. Wilson,[8] K. Abe,[9] C. Hearty,[9] T.S. Mattison,[9] J.A. McKenna,[9] D. Thiessen,[9] B. Camanzi,[10] S. Jolly,[10] A.K. McKemey,[10] J. Tinslay,[10] V.E. Blinov,[11] A.D. Bukin,[11] D.A. Bukin,[11] A.R. Buzykaev,[11] M.S. Dubrovin,[11] V.B. Golubev,[11] V.N. Ivanchenko,[11] A.A. Korol,[11] E.A. Kravchenko,[11] A.P. Onuchin,[11] A.A. Salnikov,[11] S.I. Serednyakov,[11] Yu.I. Skovpen,[11] V.I. Telnov,[11] A.N. Yushkov,[11] A.J. Lankford,[12] M. Mandelkern,[12] S. McMahon,[12] D.P. Stoker,[12] A. Ahsan,[13] K. Arisaka,[13] C. Buchanan,[13] S. Chun,[13] J.G. Branson,[14] D.B. MacFarlane,[14] S. Prell,[14] Sh. Rahatlou,[14] G. Raven,[14] V. Sharma,[14] C. Campagnari,[15] B. Dahmes,[15] P.A. Hart,[15] N. Kuznetsova,[15] S.L. Levy,[15] O. Long,[15] A. Lu,[15] J.D. Richman,[15] W. Verkerke,[15] M. Witherell,[15] S. Yellin,[15] J. Beringer,[16] D.E. Dorfan,[16] A.M. Eisner,[16] A. Frey,[16] A.A. Grillo,[16] M. Grothe,[16] C.A. Heusch,[16] R.P. Johnson,[16] W. Kroeger,[16] W.S. Lockman,[16] T. Pulliam,[16] H. Sadrozinski,[16] T. Schalk,[16] R.E. Schmitz,[16] B.A. Schumm,[16] A. Seiden,[16] M. Turri,[16] W.Walkowiak,[16] D.C. Williams,[16] M.G. Wilson,[16] E. Chen,[17] G.P. Dubois-Felsmann,[17] A. Dvoretskii,[17] D. G. Hitlin,[17] S. Metzler,[17] J. Oyang,[17] F.C. Porter,[17] A. Ryd,[17] A. Samuel,[17] M. Weaver,[17] S. Yang,[17] R.Y. Zhu,[17] S. Devmal,[18] T.L. Geld,[18] S. Jayatilleke,[18] G. Mancinelli,[18] B.T. Meadows,[18] M.D. Sokoloff,[18] P. Bloom,[19] S. Fahey,[19] W.T. Ford,[19] F. Gaede,[19] D.R. Johnson,[19] A.K. Michael,[19] U. Nauenberg,[19] A. Olivas,[19] H. Park,[19] P. Rankin,[19] J. Roy,[19] S. Sen,[19] J.G. Smith,[19] W.C. van Hoek,[19] D.L. Wagner,[19] J. Blouw,[20] J.L. Harton,[20] M. Krishnamurthy,[20] A. Soffer,[20] W.H. Toki,[20] R.J. Wilson,[20] J. Zhang,[20] T. Brandt,[21] J. Brose,[21] T. Colberg,[21] G. Dahlinger,[21] M. Dickopp,[21] R.S. Dubitzky,[21] E. Maly,[21] R. Müller-Pfefferkorn,[21] S. Otto,[21] K.R. Schubert,[21] R. Schwierz,[21] B. Spaan,[21] L. Wilden,[21] L. Behr,[22] D. Bernard,[22] G.R. Bonneaud,[22] F. Brochard,[22] J. Cohen-Tanugi,[22] S. Ferrag,[22] E. Roussot,[22] S. T'Jampens,[22] C. Thiebaux,[22] G. Vasileiadis,[22] M. Verderi,[22] A. Anjomshoaa,[23] R. Bernet,[23] F. Di Lodovico,[23] A. Khan,[23] F. Muheim,[23] S. Playfer,[23] J.E. Swain,[23] M. Falbo,[24] C. Bozzi,[25] S. Dittongo,[25] M. Folegani,[25] L. Piemontese,[25] E. Treadwell,[26] F. Anulli,[27,*] R. Baldini-Ferroli,[27] A. Calcaterra,[27] R. de Sangro,[27] D. Falciai,[27] G. Finocchiaro,[27] P. Patteri,[27] I.M. Peruzzi,[27,*] M. Piccolo,[27] Y. Xie,[27] A. Zallo,[27] S. Bagnasco,[28] A. Buzzo,[28] R. Contri,[28] G. Crosetti,[28] P. Fabbricatore,[28] S. Farinon,[28] M. Lo Vetere,[28] M. Macri,[28] M.R. Monge,[28] R. Musenich,[28] M. Pallavicini,[28] R. Parodi,[28] S. Passaggio,[28] F.C. Pastore,[28] C. Patrignani,[28] M.G. Pia,[28] C. Priano,[28] E. Robutti,[28] A. Santroni,[28] M. Morii,[29] R. Bartoldus,[30] T. Dignan,[30] R. Hamilton,[30] U. Mallik,[30] J. Cochran,[31] H.B. Crawley,[31] P.-A. Fischer,[31] J. Lamsa,[31] W.T. Meyer,[31] E.I. Rosenberg,[31] M. Benkebil,[32] G. Grosdidier,[32] C. Hast,[32] A. Höcker,[32] H.M. Lacker,[32] V. LePeltier,[32] A.M. Lutz,[32] S. Plaszczynski,[32] M.H. Schune,[32] S. Trincaz-Duvoid,[32] A. Valassi,[32] G. Wormser,[32] R.M. Bionta,[33] V. Brigljević,[33] O. Fackler,[33] D. Fujino,[33] D.J. Lange,[33] M. Mugge,[33] X. Shi,[33] K. van Bibber,[33] T.J. Wenaus,[33] D.M. Wright,[33] C.R. Wuest,[33]

M. Carroll,[34] J.R. Fry,[34] E. Gabathuler,[34] R. Gamet,[34] M. George,[34] M. Kay,[34] D.J. Payne,[34] R.J. Sloane,[34] C. Touramanis,[34] M.L. Aspinwall,[35] D.A. Bowerman,[35] P.D. Dauncey,[35] U. Egede,[35] I. Eschrich,[35] N.J.W. Gunawardane,[35] R. Martin,[35] J.A. Nash,[35] P. Sanders,[35] D. Smith,[35] D.E. Azzopardi,[36] J.J. Back,[36] P. Dixon,[36] P.F. Harrison,[36] R.J.L. Potter,[36] H.W. Shorthouse,[36] P. Strother,[36] P.B. Vidal,[36] M.I. Williams,[36] G. Cowan,[37] S. George,[37] M.G. Green,[37] A. Kurup,[37] C.E. Marker,[37] P. McGrath,[37] T.R. McMahon,[37] S. Ricciardi,[37] F. Salvatore,[37] I. Scott,[37] G. Vaitsas,[37] D. Brown,[38] C.L. Davis,[38] J. Allison,[39] R.J. Barlow,[39] J.T. Boyd,[39] A. Forti,[39] J. Fullwood,[39] F. Jackson,[39] G.D. Lafferty,[39] N. Savvas,[39] E.T. Simopoulos,[39] J.H. Weatherall,[39] A. Farbin,[40] A. Jawahery,[40] V. Lillard,[40] J. Olsen,[40] D.A. Roberts,[40] J.R. Schieck,[40] G. Blaylock,[41] C. Dallapiccola,[41] K.T. Flood,[41] S.S. Hertzbach,[41] R. Kofler,[41] C.S. Lin,[41] T.B. Moore,[41] H. Staengle,[41] S. Willocq,[41] J. Wittlin,[41] B. Brau,[42] R. Cowan,[42] G. Sciolla,[42] F. Taylor,[42] R.K. Yamamoto,[42] D.I. Britton,[43] M. Milek,[43] P.M. Patel,[43] J. Trischuk,[43] F. Lanni,[44] F. Palombo,[44] J.M. Bauer,[45] M. Booke,[45] L. Cremaldi,[45] V. Eschenberg,[45] R. Kroeger,[45] J. Reidy,[45] D.A. Sanders,[45] D.J. Summers,[45] J.P. Martin,[46] J.Y. Nief,[46] R. Seitz,[46] P. Taras,[46] V. Zacek,[46] H. Nicholson,[47] C.S. Sutton,[47] C. Cartaro,[48] N. Cavallo,[48,†] G. De Nardo,[48] F. Fabozzi,[48] C. Gatto,[48] L. Lista,[48] P. Paolucci,[48] D. Piccolo,[48] C. Sciacca,[48] J.M. LoSecco,[49] J.R.G. Alsmiller,[50] T.A. Gabriel,[50] T. Handler,[50] J. Brau,[51] R. Frey,[51] M. Iwasaki,[51] N.B. Sinev,[51] D. Strom,[51] F. Colecchia,[52] F. Dal Corso,[52] A. Dorigo,[52] F. Galeazzi,[52] M. Margoni,[52] G. Michelon,[52] M. Morandin,[52] M. Posocco,[52] M. Rotondo,[52] F. Simonetto,[52] R. Stroili,[52] E. Torassa,[52] C. Voci,[52] M. Benayoun,[53] H. Briand,[53] J. Chauveau,[53] P. David,[53] C. De la Vaissière,[53] L. Del Buono,[53] O. Hamon,[53] F. Le Diberder,[53] Ph. Leruste,[53] J. Lory,[53] L. Roos,[53] J. Stark,[53] S. Versillé,[53] P.F. Manfredi,[54] V. Re,[54] V. Speziali,[54] E.D. Frank,[55] L. Gladney,[55] Q.H. Guo,[55] J.H. Panetta,[55] C. Angelini,[56] G. Batignani,[56] S. Bettarini,[56] M. Bondioli,[56] M. Carpinelli,[56] F. Forti,[56] M.A. Giorgi,[56] A. Lusiani,[56] F. Martinez-Vidal,[56] M. Morganti,[56] N. Neri,[56] E. Paoloni,[56] M. Rama,[56] G. Rizzo,[56] F. Sandrelli,[56] G. Simi,[56] G. Triggiani,[56] J. Walsh,[56] M. Haire,[57] D. Judd,[57] K. Paick,[57] L. Turnbull,[57] D.E. Wagoner,[57] J. Albert,[58] C. Bula,[58] C. Lu,[58] K.T. McDonald,[58] V. Miftakov,[58] S.F. Schaffner,[58] A.J.S. Smith,[58] A. Tumanov,[58] E.W. Varnes,[58] G. Cavoto,[59] D. del Re,[59] R. Faccini,[14,59] F. Ferrarotto,[59] F. Ferroni,[59] K. Fratini,[59] E. Lamanna,[59] E. Leonardi,[59] M.A. Mazzoni,[59] S. Morganti,[59] G. Piredda,[59] F. Safai Tehrani,[59] M. Serra,[59] C. Voena,[59] S. Christ,[60] R. Waldi,[60] P.F. Jacques,[61] M. Kalelkar,[61] R. J. Plano,[61] T. Adye,[62] B. Franek,[62] N.I. Geddes,[62] G.P. Gopal,[62] S.M. Xella,[62] R. Aleksan,[63] G. De Domenico,[63] A. de Lesquen,[63] S. Emery,[63] A. Gaidot,[63] S.F. Ganzhur,[63] G. Hamel de Monchenault,[63] W. Kozanecki,[63] M. Langer,[63] G.W. London,[63] B. Mayer,[63] B. Serfass,[63] G. Vasseur,[63] C. Yeche,[63] M. Zito,[63] N. Copty,[64] M.V. Purohit,[64] H. Singh,[64] F.X. Yumiceva,[64] I. Adam,[65] P.L. Anthony,[65] D. Aston,[65] K. Baird,[65] J. Bartelt,[65] E. Bloom,[65] A.M. Boyarski,[65] F. Bulos,[65] G. Calderini,[65] M.R. Convery,[65] D.P. Coupal,[65] D.H. Coward,[65] J. Dorfan,[65] M. Doser,[65] W. Dunwoodie,[65] R.C. Field,[65] T. Glanzman,[65] G.L. Godfrey,[65] P. Grosso,[65] T. Himel,[65] M.E. Huffer,[65] W.R. Innes,[65] C.P. Jessop,[65] M.H. Kelsey,[65] P. Kim,[65] M.L. Kocian,[65] U. Langenegger,[65] D.W.G.S. Leith,[65] S. Luitz,[65] V. Luth,[65] H.L. Lynch,[65] G. Manzin,[65] H. Marsiske,[65] S. Menke,[65] R. Messner,[65] K.C. Moffeit,[65] R. Mount,[65] D.R. Muller,[65] C.P. O'Grady,[65] S. Petrak,[65] H. Quinn,[65] B.N. Ratcliff,[65] S.H. Robertson,[65] L.S. Rochester,[65] A. Roodman,[65] T. Schietinger,[65] R.H. Schindler,[65] J. Schwiening,[65] V.V. Serbo,[65] A. Snyder,[65] A. Soha,[65] S.M. Spanier,[65] A. Stahl,[65] J. Stelzer,[65] D. Su,[65] M.K. Sullivan,[65] M. Talby,[65] H.A. Tanaka,[65] A. Trunov,[65] J. Va'vra,[65] S. R. Wagner,[65] A.J.R. Weinstein,[65] W.J. Wisniewski,[65] C.C. Young,[65] P.R. Burchat,[66] C.H. Cheng,[66] D. Kirkby,[66] T.I. Meyer,[66] C. Roat,[66] R. Henderson,[67] W. Bugg,[68] H. Cohn,[68] E. Hart,[68] A.W. Weidemann,[68] T. Benninger,[69] J.M. Izen,[69] I. Kitayama,[69] X.C. Lou,[69] M. Turcotte,[69] F. Bianchi,[70] M. Bona,[70] B. Di Girolamo,[70] D. Gamba,[70] A. Smol,[70] D. Zanin,[70] L. Bosisio,[71] G. Della Ricca,[71] L. Lanceri,[71] A. Pompili,[71] P. Poropat,[71] M. Prest,[71] E. Vallazza,[71] G. Vuagnin,[71] R.S. Panvini,[72] C.M. Brown,[73] A. De Silva,[73] R. Kowalewski,[73] J.M. Roney,[73] H.R. Band,[74] E. Charles,[74] S. Dasu,[74] P. Elmer,[74] H. Hu,[74] J.R. Johnson,[74] R. Liu,[74] J. Nielsen,[74] W. Orejudos,[74] Y. Pan,[74] R. Prepost,[74] I.J. Scott,[74] S.J. Sekula,[74] J.H. von Wimmersperg-Toeller,[74] S.L. Wu,[74] Z. Yu,[74] H. Zobernig,[74] T.M.B. Kordich,[75] and H. Neal[75]

[1] *Laboratoire de Physique des Particules, F-74941 Annecy-le-Vieux, France*
[2] *Università di Bari, Dipartimento di Fisica and INFN, I-70126 Bari, Italy*
[3] *Institute of High Energy Physics, Beijing 100039, China*
[4] *University of Bergen, Inst. of Physics, N-5007 Bergen, Norway*
[5] *Lawrence Berkeley National Laboratory and University of California, Berkeley, CA 94720, USA*
[6] *University of Birmingham, Birmingham, B15 2TT, UK*
[7] *Ruhr Universität Bochum, Institut für Experimentalphysik 1, D-44780 Bochum, Germany*
[8] *University of Bristol, Bristol BS8 lTL, UK*

[9] *University of British Columbia, Vancouver, BC, Canada V6T 1Z1*
[10] *Brunel University, Uxbridge, Middlesex UB8 3PH, UK*
[11] *Budker Institute of Nuclear Physics, Novosibirsk 630090, Russia*
[12] *University of California at Irvine, Irvine, CA 92697, USA*
[13] *University of California at Los Angeles, Los Angeles, CA 90024, USA*
[14] *University of California at San Diego, La Jolla, CA 92093, USA*
[15] *University of California at Santa Barbara, Santa Barbara, CA 93106, USA*
[16] *University of California at Santa Cruz, Institute for Particle Physics, Santa Cruz, CA 95064, USA*
[17] *California Institute of Technology, Pasadena, CA 91125, USA*
[18] *University of Cincinnati, Cincinnati, OH 45221, USA*
[19] *University of Colorado, Boulder, CO 80309, USA*
[20] *Colorado State University, Fort Collins, CO 80523, USA*
[21] *Technische Universität Dresden, Institut für Kern-und Teilchenphysik, D-0l062,Dresden, Germany*
[22] *Ecole Polytechnique, F-91128 Palaiseau, France*
[23] *University of Edinburgh, Edinburgh EH9 3JZ, UK*
[24] *Elon College, Elon College, NC 27244-2010, USA*
[25] *Università di Ferrara, Dipartimento di Fisica and INFN, I-44100 Ferrara, Italy*
[26] *Florida A&M University, Tallahassee, FL 32307, USA*
[27] *Laboratori Nazionali di Frascati dell'INFN, I-00044 Frascati, Italy*
[28] *Università di Genova, Dipartimento di Fisica and INFN, I-16146 Genova, Italy*
[29] *Harvard University, Cambridge, MA 02138, USA*
[30] *University of Iowa, Iowa City, IA 52242, USA*
[31] *Iowa State University, Ames, IA 50011-3160, USA*
[32] *Laboratoire de l'Accélérateur Linéaire, F-91898 Orsay, France*
[33] *Lawrence Livermore National Laboratory, Livermore, CA 94550, USA*
[34] *University of Liverpool, Liverpool L69 3BX, UK*
[35] *University of London, Imperial College, London SW7 2BW, UK*
[36] *Queen Mary, University of London, London E1 4NS, UK*
[37] *University of London, Royal Holloway and Bedford New College, Egham, Surrey TW20 0EX, UK*
[38] *University of Louisville, Louisville, KY 40292, USA*
[39] *University of Manchester, Manchester M13 9PL, UK*
[40] *University of Maryland, College Park, MD 20742, USA*
[41] *University of Massachusetts, Amherst, MA 01003, USA*
[42] *Massachusetts Institute of Technology, Lab for Nuclear Science, Cambridge, MA 02139, USA*
[43] *McGill University, Montréal, QC, Canada H3A 2T8*
[44] *Università di Milano, Dipartimento di Fisica and INFN, I-20133 Milano, Italy*
[45] *University of Mississippi, University, MS 38677, USA*
[46] *Université de Montréal, Lab. René J. A. Levesque, Montréal, QC, Canada, H3C 3J7*
[47] *Mount Holyoke College, South Hadley, MA 01075, USA*
[48] *Università di Napoli Federico II, Dipartimento di Scienze Fishiche and INFN, I-80126, Napoli, Italy*
[49] *University of Notre Dame, Notre Dame, IN 46556, USA*
[50] *Oak Ridge National Laboratory, Oak Ridge, TN 37831, USA*
[51] *University of Oregon, Eugene, OR 97403, USA*
[52] *Università di Padova, Dipartimento di Fisica and INFN, I-35131 Padova, Italy*
[53] *Universités Paris VI et VII, Lab de Physique Nucléaire H. E., F-75252 Paris, France*
[54] *Università di Pavia, Dipartimento di Elettronica and INFN, I-27100 Pavia, Italy*
[55] *University of Pennsylvania, Philadelphia, PA 19104, USA*
[56] *Università di Pisa, Scuola Normale Superiore, and INFN, I-56010 Pisa, Italy*
[57] *Prairie View A&M University, Prairie View, TX 77446, USA*
[58] *Princeton University, Princeton, NJ 08544, USA*
[59] *Università di Roma La Sapienza, Dipartimento di Fisica and INFN, I-00185 Roma, Italy*
[60] *Universität Rostock, D-18051 Rostock, Germany*
[61] *Rutgers University, New Brunswick, NJ 08903, USA*
[62] *Rutherford Appleton Laboratory, Chilton, Didcot, Oxon, OX11 0QX, UK*
[63] *DAPNIA, Commissariat à l'Energie Atomique/Saclay, F-91191 Gif-sur-Yvette, France*
[64] *University of South Carolina, Columbia, SC 29208, USA*
[65] *Stanford Linear Accelerator Center, Stanford, CA 94309, USA*
[66] *Stanford University, Stanford, CA 94305-4060, USA*
[67] *TRIUMF, Vancouver, BC, Canada V6T 2A3*
[68] *University of Tennessee, Knoxville, TN 37996, USA*
[69] *University of Texas at Dallas, Richardson, TX 75083, USA*
[70] *Università di Torino, Dipartimento di Fisica Sperimentale and INFN, I-10125 Torino, Italy*
[71] *Università di Trieste, Dipartimento di Fisica and INFN, I-34127 Trieste, Italy*
[72] *Vanderbilt University, Nashville, TN 37235, USA*

[73] University of Victoria, Victoria, BC, Canada V8W 3P6
[74] University of Wisconsin, Madison, WI 53706, USA
[75] Yale University, New Haven, CT 06511, USA

(Dated: March 29, 2001)

We have observed the decays $B \to \phi K$ and $\phi K^*$ in a sample of over 45 million $B$ mesons collected with the *BABAR* detector at the PEP-II collider. The measured branching fractions are $\mathcal{B}(B^+ \to \phi K^+) = (7.7^{+1.6}_{-1.4} \pm 0.8) \times 10^{-6}$, $\mathcal{B}(B^0 \to \phi K^0) = (8.1^{+3.1}_{-2.5} \pm 0.8) \times 10^{-6}$, $\mathcal{B}(B^+ \to \phi K^{*+}) = (9.7^{+4.2}_{-3.4} \pm 1.7) \times 10^{-6}$, and $\mathcal{B}(B^0 \to \phi K^{*0}) = (8.6^{+2.8}_{-2.4} \pm 1.1) \times 10^{-6}$. We also report the upper limit $\mathcal{B}(B^+ \to \phi\pi^+) < 1.4 \times 10^{-6}$ (90% CL).

PACS numbers: 13.25.Hw, 13.25.-k, 14.40.Nd

The decays of $B$ mesons into charmless hadronic final states provide important information for the study of $CP$ violation and the search for new physics. Decays into final states containing a $\phi$ meson are particularly interesting because they are dominated by $b \to s(d)\bar{s}s$ penguins (Fig. 1), with gluonic and electroweak contributions, while other Standard Model contributions are highly suppressed [1]. These modes thus provide a direct measurement of the penguin process, with potential benefits to estimates of direct $CP$ violation. They also allow an independent measurement of $\sin 2\beta$ [2]. Comparison of the value of $\sin 2\beta$ obtained from these modes with that from charmonium modes, as well as various tests of isospin relationships, can probe for new physics [3, 4].

In this paper we present measurements of four such decays: $B^+ \to \phi K^+$, $B^0 \to \phi K^0$, $B^+ \to \phi K^{*+}$, and $B^0 \to \phi K^{*0}$. Charge conjugate states are assumed throughout this paper and measured branching fractions are averaged accordingly. The $\phi K^+$ and $\phi K^{*0}$ modes have been previously seen [5].

The data were collected with the *BABAR* detector [6] at the PEP-II asymmetric $e^+e^-$ collider [7] located at the Stanford Linear Accelerator Center. The results presented in this paper are based on data taken in the 1999–2000 run. An integrated luminosity of 20.7 fb$^{-1}$ was recorded corresponding to 22.7 million $B\overline{B}$ pairs at the $\Upsilon(4S)$ resonance ("on-resonance") and 2.6 fb$^{-1}$ about 40 MeV below this energy ("off-resonance").

The asymmetric beam configuration in the laboratory frame provides a boost to the $\Upsilon(4S)$ increasing the momentum range of the $B$-meson decay products up to

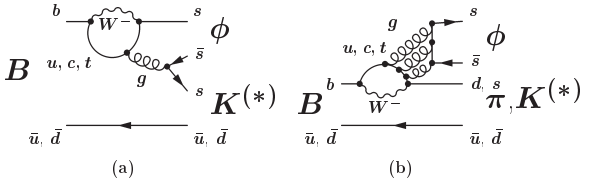


FIG. 1: Gluonic penguin diagrams describing the decays $B \to \phi K$, $\phi K^*$, and $\phi\pi$: (a) internal (b) flavor-singlet.

4.3 GeV/$c$. Charged particles are detected and their momenta are measured by a combination of a silicon vertex tracker (SVT) consisting of five double-sided layers and a 40-layer central drift chamber (DCH), both operating in a 1.5 T solenoidal magnetic field. With the SVT, a position resolution of about 40 $\mu$m is achieved for the highest momentum charged particles near the interaction point, allowing the precise determination of decay vertices. The tracking system covers 92% of the solid angle in the center-of-mass system (CM). The track finding efficiency is, on average, (98±1)% for momenta above 0.2 GeV/$c$ and polar angle greater than 0.5 rad. Photons are detected by a CsI electromagnetic calorimeter (EMC), which provides excellent angular and energy resolution with high efficiency for energies above 20 MeV [6].

Charged particle identification is provided by the average energy loss ($dE/dx$) in the tracking devices and by a unique, internally reflecting ring imaging Cherenkov detector (DIRC) covering the central region. A Cherenkov angle $K$–$\pi$ separation of better than $4\sigma$ is achieved for tracks below 3 GeV/$c$ momentum, decreasing to $2.5\sigma$ at the highest momenta in our final states. Electrons are identified with the use of the EMC.

Hadronic events are selected based on track multiplicity and event topology. We fully reconstruct $B$ meson candidates from their charged and neutral decay products, where we recover the intermediate states $\pi^0 \to \gamma\gamma$, $K^0 \to K^0_S \to \pi^+\pi^-$, $\phi \to K^+K^-$, $K^{*+} \to K^0\pi^+$ or $K^+\pi^0$, and $K^{*0} \to K^+\pi^-$. Candidate charged tracks are required to originate from the interaction point (within 10 cm along the beam direction and 1.5 cm in the transverse plane), and to have at least 12 DCH hits and a minimum transverse momentum of 0.1 GeV/$c$. Looser criteria are applied to tracks forming $K^0_S$ candidates to allow for displaced decay vertices. Kaon tracks are distinguished from pion and proton tracks via a likelihood ratio that includes, for momenta below 0.7 GeV/$c$, $dE/dx$ information from the SVT and DCH, and, for higher momenta, the Cherenkov angle and number of photons as measured by the DIRC. A kaon (pion) candidate is any track not identified as a proton or pion (kaon).

We reconstruct $\pi^0$ mesons as pairs of photons with a minimum energy deposition of 30 MeV. The typical width of the reconstructed $\pi^0$ mass is 7 MeV/$c^2$. A

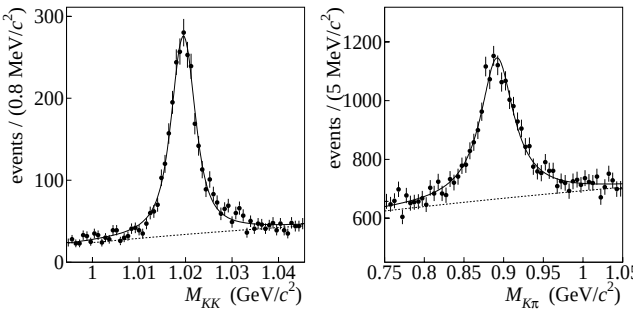


FIG. 2: The two-kaon invariant mass in the $\phi$ signal region (left). Superimposed to the data is the fit to a relativistic $P$-wave Breit-Wigner for the $\phi$ convoluted with a Gaussian on top of a polynomial background. The mass resolution is 1.1 MeV/$c^2$. The plot to the right shows a Breit-Wigner fit to the $K^0\pi^+$ invariant mass in the $K^{*+}$ signal region. Both fits use Breit-Wigner parameters from Ref. [8].

$\pm 15$ MeV/$c^2$ interval is applied to select $\pi^0$ candidates.

We combine pairs of tracks with opposite charge from a common vertex to form $K^0_S$, $\phi$, and $K^{*0}$ candidates. The selection of $K^0_S$ candidates is based on the invariant two-pion mass ($|M_{\pi\pi} - m_{K^0}| < 10$ MeV/$c^2$), the angle $\alpha$ between the reconstructed flight and momentum directions in the plane transverse to the beam direction ($\cos\alpha > 0.999$), and the measured lifetime significance ($\tau/\sigma_\tau > 3$). For the softer $K^0_S$ from $K^{*+}$ decays we relax the criteria to 12 MeV/$c^2$ and $\cos\alpha > 0.995$.

For $\phi$ candidates, both daughters are required to be kaon candidates. The invariant mass for the $K^+K^-$ pair must lie within 30 MeV/$c^2$ of the $\phi$ mass (see Fig. 2).

The natural width of the $K^*$ dominates the resolution in the invariant mass spectrum. For $K^{*0}$ candidates the $K\pi$ invariant mass interval is $\pm 100$ MeV/$c^2$. The selection of $K^{*+}$ comprises $K^+\pi^0$ and $K^0_S\pi^+$ combinations within a $K\pi$ mass interval of $\pm 150$ MeV/$c^2$ (see Fig. 2). We require particle identification for the charged daughters of the $K^*$. To suppress combinatorial background we restrict the $K^{*+} \to K^+\pi^0$ helicity angle ($\cos\theta_H > -0.5$ as defined below). This effectively requires the $\pi^0$ momentum to be above 0.35 GeV/$c$.

The helicity angle $\theta_H$ of a $\phi$ or $K^*$ is defined as the angle between one resonance daughter direction and the parent $B$ direction in the resonance rest frame. For pseudoscalar-vector $B$ decay modes, angular momentum conservation results in a $\cos^2\theta_H$ distribution, whereas in decays into vector-vector states, the distribution is the result of an *a priori* unknown superposition of transverse and longitudinal polarizations.

We identify $B$ meson candidates kinematically using two independent variables [6], $\Delta E = (E_i E_B - \mathbf{p}_i\cdot\mathbf{p}_B - s/2)/\sqrt{s}$ and the energy-substituted mass $m_{\rm ES} = \sqrt{(s/2 + \mathbf{p}_i\cdot\mathbf{p}_B)^2/E_i^2 - \mathbf{p}_B^2}$, where $\sqrt{s}$ is the total $e^+e^-$ CM energy. The initial state four-momentum $(E_i, \mathbf{p}_i)$ derived from the beam kinematics and the four-momentum $(E_B, \mathbf{p}_B)$ of the reconstructed $B$ candidate are all defined in the laboratory. The calculation of $m_{\rm ES}$ only involves the three-momenta of the decay products, and is therefore independent of the masses assigned to them. For signal events $\Delta E$ peaks at zero and $m_{\rm ES}$ at the $B$ mass. Our initial selection requires $|\Delta E| < 0.23$ GeV and $m_{\rm ES} > 5.2$ GeV/$c^2$.

Monte Carlo (MC) simulation [10] demonstrates that contamination from other $B$ decays is negligible. However, charmless hadronic modes suffer from large backgrounds due to random combinations of tracks produced in the quark-antiquark ($q\bar{q}$) continuum. The distinguishing feature of such backgrounds is their characteristic event shape resulting from the two-jet production mechanism. We have considered a variety of event shape variables in the CM that exploit this difference.

One such variable is the angle $\theta_T$ between the thrust axis of the $B$ candidate and the thrust axis of the rest of the event, where the thrust axis is defined as the axis that maximizes the sum of the magnitudes of the longitudinal momenta. This angle is small for continuum events, where the $B$-candidate daughters tend to lie in the $q\bar{q}$ jets, and uniformly distributed for true $B\overline{B}$ events. Thus we require $|\cos\theta_T| < 0.9$ (0.8 for $\phi K^{*+}$).

Other quantities that characterize the event shape are the $B$ polar angle $\theta_B$ and the angle $\theta_{q\bar{q}}$ of the $B$-candidate thrust axis, both defined with respect to the beam axis, as well as the angular energy flow of the charged particles and photons relative to the $B$-candidate thrust axis. For $\Upsilon(4S)$ decays into two pseudoscalar $B$ mesons, the $\theta_B$ distribution has a $\sin^2\theta_B$ dependence, whereas the jets from continuum events lead to a uniform distribution in $\cos\theta_B$. In $\theta_{q\bar{q}}$, the continuum jets give rise to a $(1 + \cos^2\theta_{q\bar{q}})$ distribution, while the thrust direction of true $B$ decays is random. We enhance the background suppression by forming an optimized linear combination of eleven variables (Fisher discriminant): $|\cos\theta_B|$, $|\cos\theta_{q\bar{q}}|$, and energy flow into the nine 10° polar angle intervals coaxial around the $B$ candidate thrust axis [9].

We use an extended unbinned maximum likelihood (ML) fit to extract signal yields. The extended likelihood for a sample of $N$ events is

$$\mathcal{L} = \exp\left(-\sum_{i=1}^{M} n_i\right) \prod_{j=1}^{N} \left(\sum_{i=1}^{M} n_i\, \mathcal{P}_i(\vec{x}_j;\vec{\alpha})\right), \quad (1)$$

where $\mathcal{P}_i(\vec{x}_j;\vec{\alpha})$ describes the probability for candidate event $j$ to belong to category $i$, based on its measured variables $\vec{x}_j$, and fixed parameters $\vec{\alpha}$ that describe the expected distributions of these variables in each of the $M$ categories. In the simplest case, the probabilities are summed over two categories ($M = 2$), signal and background. The decays $B^+ \to \phi K^+$ and $B^+ \to \phi\pi^+$ are fit simultaneously with two signal and two corresponding background categories ($M = 4$). The event yields $n_i$

in each category are obtained by maximizing $\mathcal{L}$ [11]. Statistical errors correspond to unit changes in the quantity $\chi^2 = -2\ln\mathcal{L}$ around its minimum value. The significance of a signal is defined by the square root of the change in $\chi^2$ when constraining the number of signal events to zero in the likelihood fit.

The probability $\mathcal{P}_i(\vec{x}_j;\vec{\alpha})$ for a given event $j$ is the product of independent probability density functions (PDFs) in each of the fit input variables $\vec{x}_j$. These are $\Delta E$, $m_{\rm ES}$, $M_{KK}$ for all channels, $M_{K\pi}$ for the $\phi K^*$ channels, the $\phi$ helicity angle for pseudoscalar-vector decays, and event shape quantities as discussed below. For the simultaneous fit to the decays $B^+ \to \phi K^+$ and $\phi\pi^+$ we include normalized residuals derived from the difference between measured and expected DIRC Cherenkov angles for the charged primary daughter. Additional separation between the two final states is provided by $\Delta E$.

The fixed parameters $\vec{\alpha}$ describing the PDFs are extracted from signal and background distributions from MC simulation, on-resonance $\Delta E$–$m_{\rm ES}$ sidebands, and off-resonance data. The MC resolutions are adjusted by comparisons of data and simulation in abundant calibration channels with similar kinematics and topology, such as $B \to D\pi, D\rho$ with $D \to K\pi, K\pi\pi$. The simulation reproduces the event-shape variable distributions found in data. The Cherenkov angle residual parameterizations are determined from samples of $D^0 \to K^-\pi^+$ originating from $D^*$ decays.

For the parameterization of the PDFs for $\Delta E$, $m_{\rm ES}$, and resonance masses we employ Gaussian and Breit-Wigner functions to describe the signal distributions. For the background we use low-degree polynomials or, in the case of $m_{\rm ES}$, an empirical phase-space function [12]. The background parameterizations for $M_{KK}$ and $M_{K\pi}$ also include a resonant component to account for $\phi$ and $K^*$ production in the continuum. The $\phi K$ ($\phi\pi$) helicity-angle distribution is assumed to be $\cos^2\theta_H$ for signal. The background shape is again separated into contributions from combinatorics and from real $\phi$ mesons, both fit by nearly constant low-degree polynomials. The Cherenkov angle residual PDFs are Gaussian for both the pion and kaon distributions. The thrust and production angle PDFs are parameterized by polynomials, with the exception of the background in $|\cos\theta_T|$, where we use an exponential. The Fisher discriminant is described by an asymmetric Gaussian for both signal and background.

For all modes, we test the fit response for various choices of preselection and fit strategies with samples generated according to the PDFs, each containing the expected number of events in signal and background. Signal yields were found to be unbiased. In the $\phi K^0$ analysis the results of our tests show that fitting either to $|\cos\theta_T|$ and $\cos\theta_B$ or to the Fisher discriminant yields comparable significance. Thus, we use only the thrust and $B$ polar angle in this analysis. In the other modes we find that the additional background discrimination provided by the Fisher discriminant improves the expected significances of the results, and use this approach.

TABLE I: Summary of results; $\varepsilon$ denotes the reconstruction efficiency and $\varepsilon_{\rm tot}$ the total efficiency including daughter branching fractions, both in percent; $N$ is the number of events entering the ML fit, $n_{\rm sig}$ the fitted number of signal events, $S$ the statistical significance (in Gaussian $\sigma$), and $\mathcal{B}$ the measured branching fraction including statistical and systematic errors. The subscripts in the $\phi K^{*+}$ modes refer to the kaon daughter of the $K^{*+}$.

| Mode | $\varepsilon$ | $\varepsilon_{\rm tot}$ | $N$ | $n_{\rm sig}$ | $S$ | $\mathcal{B}(10^{-6})$ |
|---|---|---|---|---|---|---|
| $\phi K^+$ | 36.4 | 17.9 | 4202 | $31.4^{+6.7}_{-5.9}$ | 10.5 | $7.7^{+1.6}_{-1.4} \pm 0.8$ |
| $\phi K^0$ | 37.4 | 6.1 | 351 | $10.8^{+4.1}_{-3.3}$ | 6.4 | $8.1^{+3.1}_{-2.5} \pm 0.8$ |
| $\phi K^{*+}$ | – | 4.9 | – | – | 4.5 | $9.7^{+4.2}_{-3.4} \pm 1.7$ |
| $\phi K^{*+}_{K^+}$ | 15.1 | 2.5 | 781 | $7.1^{+4.3}_{-3.4}$ | 2.7 | $12.8^{+7.7}_{-6.1} \pm 3.2$ |
| $\phi K^{*+}_{K^0}$ | 21.5 | 2.4 | 381 | $4.4^{+2.7}_{-2.0}$ | 3.6 | $8.0^{+5.0}_{-3.7} \pm 1.3$ |
| $\phi K^{*0}$ | 26.3 | 8.6 | 2517 | $16.9^{+5.5}_{-4.7}$ | 6.6 | $8.6^{+2.8}_{-2.4} \pm 1.1$ |
| $\phi\pi^+$ | 38.9 | 19.1 | 4202 | $0.9^{+2.1}_{-0.9}$ | 0.6 | $< 1.4$ (90% CL) |

The results of our ML fit analyses are summarized in Table I. For the branching fractions we assume equal production rates of $B^0\overline{B}^0$ and $B^+B^-$. We find significant signals in all four $B \to \phi K$ and $\phi K^*$ decay modes. The number of fit events, their statistical significance, and the ML fit $\chi^2$ values are well reproduced with generated samples. Projections of the input variables are in good agreement with the fit results, as shown for $m_{\rm ES}$ in Fig. 3.

We check the stability of our results by reducing the number of input variables in the fit. In particular, we find statistically significant signals even if event shape variables are omitted from the fit and only preselection criteria are required. Correlations among the input variables are found to be less than 10%.

Systematic uncertainties in the ML fit originate from assumptions about the signal and background distributions. We vary the PDF parameters within their respective uncertainties, and derive the associated systematic errors. They range between 4 and 9% (17% for the final state that includes a $\pi^0$). The signals remain statistically significant within these variations.

The dominant systematic errors in the efficiency are track finding (1.2% per track), particle identification (2% per track), and $K^0_S$ and $\pi^0$ reconstruction (7% and 5%, respectively). Other minor systematic effects from event selection criteria, daughter branching fractions, MC statistics, and $B$ meson counting sum to less than 4%. The efficiency in the ML fit to signal samples can be less than 100% because of fake combinations passing the selection criteria, and we account for this with a systematic uncertainty (2–5%). This effect is larger in the $K^*$ final states because of broader distributions and combinatorial $\pi^0$ background. Uncertainties in the efficiency only

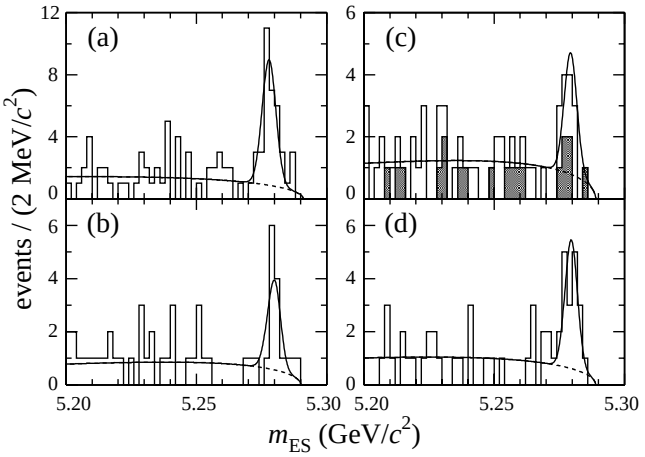


FIG. 3: Projections onto the variable $m_{\rm ES}$. The histograms show data for (a) $B^+ \to \phi K^+$; (b) $B^0 \to \phi K^0$; (c) $B^+ \to \phi K^{*+}$; (d) $B^0 \to \phi K^{*0}$ after a requirement on the signal probability $\mathcal{P}_{\rm sig}/\Sigma\mathcal{P}_i$ with the PDF for $m_{\rm ES}$ excluded. In (c) the histogram is the sum of the two $\phi K^{*+}$ channels while the shaded area is $K^{*+} \to K^0\pi^+$ alone. The solid (dashed) line shows the PDF projection of the full fit (background only).

affect the branching fraction, but not the significance of a result.

In the vector-vector final states we average efficiencies for the transverse and longitudinal angular polarizations and assign a systematic error as the rms spread of a uniform efficiency distribution between the two extreme cases (6% in $\phi K^{*+}_{K^0}$, 14% in $\phi K^{*+}_{K^+}$, and 2% in $\phi K^{*0}$). We combine the results from the two $K^{*+}$ decay channels using $\chi^2$ distributions convoluted with the uncorrelated part of the systematic errors.

The fit result for the $B^+ \to \phi\pi^+$ branching fraction is $(2.1^{+4.9}_{-2.1} \pm 0.5) \times 10^{-7}$. Given the signal yield of less than one event, we quote an upper limit obtained by integrating the normalized likelihood distribution. The limit incorporates changes by one standard deviation from uncertainties in PDFs and the reconstruction efficiency.

Event counting analyses, based on the same variable set $x_j$ as used in the fits, serve as cross-checks for the ML fit results. The variable ranges are generally chosen to be tighter in order to optimize the signal-to-background ratio, or upper limit, for the expected branching fractions. We count events in a rectangular signal region in the $\Delta E$–$m_{\rm ES}$ plane, and estimate the background from a sideband area. For $B^+ \to \phi K^+$ we find 43 events in the signal region (expected background 9.4); the corresponding numbers are 10 (2.8) for $\phi K^0$, 6 (2.2) for $\phi K^{*+}$, 22 (7.3) for $\phi K^{*0}$, and 2 (3) for $\phi\pi^+$. The branching fractions measured using this technique are in good agreement with those arising from the ML fit analysis.

In summary, we have observed $B$ decays to $\phi K^+$, $\phi K^0$, $\phi K^{*+}$, and $\phi K^{*0}$ with significances, including systematic uncertainties, of greater than four standard deviations (Table I). The agreement between the branching fractions of charged and neutral modes is in accordance with isospin invariance under the assumption of penguin diagram dominance. The decay $B^+ \to \phi\pi^+$ has both CKM and color suppression relative to $\phi K^+$ [4] and is therefore not expected to be observed in the present data sample.

We are grateful for the extraordinary contributions of our PEP-II colleagues in achieving the excellent luminosity and machine conditions that have made this work possible. The collaborating institutions wish to thank SLAC for its support and the kind hospitality extended to them. This work is supported by the the US Department of Energy and National Science Foundation, the Natural Sciences and Engineering Research Council (Canada), Institute of High Energy Physics (China), the Commissariat à l'Energie Atomique and Institut National de Physique Nucléaire et de Physique des Particules (France), the Bundesministerium für Bildung und Forschung (Germany), the Istituto Nazionale di Fisica Nucleare (Italy), the Research Council of Norway, the Ministry of Science and Technology of the Russian Federation, and the Particle Physics and Astronomy Research Council (United Kingdom). Individuals have received support from the Swiss National Science Foundation, the A. P. Sloan Foundation, the Research Corporation, and the Alexander von Humboldt Foundation.

---

* Also with Università di Perugia, Perugia, Italy.
† Also with Università della Basilicata, Potenza, Italy.

[1] N.G. Deshpande and J. Trampetic, Phys. Rev. D **41**, 895 (1990); N.G. Deshpande and X.-G. He, Phys. Lett. B **336**, 471 (1994); R. Fleischer, Z. Phys. C **62**, 81 (1994).
[2] I. Dunietz and J.L. Rosner, Phys. Rev. D **34**, 1404 (1986).
[3] Y. Grossman and M.P. Worah, Phys. Lett. B **395**, 241 (1997).
[4] R. Fleischer, Int. J. Mod. Phys. A **12**, 2459 (1997).
[5] CLEO Collaboration, preprint hep-ex/0101032, submitted to Phys. Rev. Lett.
[6] *BABAR* Collaboration, B. Aubert *et al.*, SLAC-PUB-8569, submitted to Nucl. Instrum. and Methods.
[7] PEP-II Conceptual Design Report, SLAC-R-418 (1993).
[8] Particle Data Group, D.E. Groom *et al.*, Eur. Phys. J. C **15**, 1 (2000).
[9] CLEO Collaboration, D.M. Asner *et al.*, Phys. Rev. D **53**, 1039 (1996).
[10] The *BABAR* detector Monte Carlo simulation is based on GEANT: R. Brun *et al.*, CERN DD/EE/84-1.
[11] F. James, CERN Program Library, D506.
[12] ARGUS Collaboration, H. Albrecht *et al.*, Phys. Lett. B **241**, 278 (1990).